European Food Research and Technology (2023) 249:1125–1136
https://doi.org/10.1007/s00217-023-04202-3

ORIGINAL PAPER

Development of a magnetic separation immunoassay with high sensitivity and time-saving for detecting aflatoxin B_1 in agricultural crops using nanobody

Xinyang Wang[1,2] · Wentao Liu[4] · Hu Zuo[2] · Weili Shen[1,2] · Yiyang Zhang[2] · Ruonan Liu[2] · Lu Geng[2] · Wen Wang[2] · Changli Shao[1,3] · Tieqiang Sun[2]

Received: 29 October 2022 / Revised: 6 January 2023 / Accepted: 7 January 2023 / Published online: 3 February 2023

Abstract

Detection methods with high sensitivity and short assay time are urgently required for quantitative analysis of small-molecule hazardous substances in food monitoring. In this work, a new anti-aflatoxin B_1 (AFB_1) nanobody was screened from an immunized nanobody library, and an ultrafast one-step detection of AFB_1 without immobilization and multi-step washing was developed based on magnetic separation technology and nanobody (Nb)-alkaline phosphatase (ALP) fusion protein. Compared to conventional one-step chemiluminescent enzyme-linked immunosorbent assay (CLEIA) based on Nb-ALP, it was surprising to find the sensitivity and lowest limit of detection (LOD) of this method was significantly improved about threefold and fivefold separately, and the total assay time could be reduced to 30 from 120 min. Under optimal conditions, the developed method achieved the sensitive detection of AFB_1 with LOD with 0.743 pg mL^{-1}, IC_{50} = 0.33 ng mL^{-1}, the linear range was 7.23 pg mL^{-1} ~ 12.38 ng mL^{-1}, and showed powerful tolerance and utility for complex matrix environments in sample detection. It is believed this method could provide a newly way for the quick and sensitive detection of AFB_1 and could expand the application of Nbs.

Keywords AFB_1 · Nanobody · Alkaline phosphatase · Magnetic separation · Chemiluminescence immunoassay

Introduction

Aflatoxin B_1 (AFB_1) is well known for its toxicity and one of the most toxic of over 20 types of aflatoxins that have been found, and its contamination is mostly found in tropical and subtropical regions [1]. However, due to changes in climatic environment, the regional distribution of AFB_1 contamination may increase in future years, and this also means that the pollution could be triggered in many environments that are so far safe [2, 3]. Numerous studies have proven that long-term exposure to AFB_1 contamination could cause cancer, birth defects, chronic toxicity or even genetic alterations in human beings, and huge economic losses follow [4]. Because of the lack of efficient and stable means of detoxification, the accumulation of food chain has become the main pathway causing above problems [5, 6]. Therefore, the necessity of rapid detection capability is magnified, such rapid and quantitative analysis is critical to offer real-time monitoring and early warning.

Significant effort has gone into and attainments have been achieved for AFB_1 detection by liquid chromatography-tandem mass spectrometry, high-performance liquid chromatography and employing thin layer chromatography [7–9]. Nevertheless, the above methods require time-consuming pre-processing steps and specialized testing instruments, which limit the rapid and timely quantitative analysis of

✉ Changli Shao
shaochl@126.com

✉ Tieqiang Sun
suntq106@163.com

1 Department of Immunology, School of Basic Medicine, Jiamusi University, Jiamusi , Heilongjiang, China

2 Tianjin Key Laboratory of Risk Assessment and Control Technology for Environment and Food Safety, Tianjin Institute of Environmental and Operational Medicine, Tianjin, China

3 Key Laboratory of Microecology-Immune Regulatory Network and Related Diseases, School of Basic Medicine, Jiamusi University, Jiamusi, Heilongjiang Province, China

4 School of Information Science and Engineering, Xinjiang University, Xinjiang, China

AFB_1 to varying degrees. Immunoassay that applies specific binding of antibody (Ab) and antigen (Ag) has been favored and widely utilized thanks to its superiorities of high sensitivity, universal application, low cost and easy operation [10–12]. Traditional immunoassay-based enzyme-linked immunosorbent assay (ELISA) or chemiluminescent enzyme-linked immunosorbent assay (CLEIA) require cumbersomely repetitive operation and enzyme-labeled-antibody, which lengthen the detection time and the analytical errors. Those bottleneck problem hinders the further development of immunoassay. Easier operate, less time cost, better performance detection method is urgently needed.

Traditional immunoassay mainly developed by monoclonal antibodies or polyclonal antibodies, usually need to be chemically labeled with biotin [13], fluorescent molecule or nanomaterials [14], which could improve the performance, while multifarious steps, loss of activity, difference between batch still cannot be avoided [15]. Nanobody (Nb), the variable domain of heavy chain antibody, is a fragment derived from the camelid antibody, the smallest antibody [16], which endows with excellent stability, easy genetic-operability and easy preparation, which would be a better way to upgrade the immunoassay. Some feasible one-step immunoassay methods have been developed using Nb-fusion proteins, which could reduce detection time and improve sensitivity [17, 18]. For AFB_1 detection, some methods based on Nb and their fusion protein have been developed [19], which also were restricted with longer detection time (about 50 min), narrower detection range and complex process, as antigen immobilization, blocking process and inefficient signal out strategy are still unsolved. Magnetic beads (MBs) possessed low production cost, easy modification, good biocompatibility, environmental harmlessness, would be used as an alternative immobilization support and provide a "mix and read" method for AFB_1 detection, magnetic bead-based immunoassay (MB-IA), which would provide a homogeneous liquid phase reaction environment for the reaction of antigen and antibody [20, 21]. What is more, most food and environmental samples intrinsically have a low magnetic background, and there would be only simple or even no pretreatment process in actual sample testing while not compromising the sensitivity [22].

Here, an AFB_1·BSA-MB and anti-AFB_1 alkaline phosphatase-nanobody (ALP-Nb) fusion protein-based one-step chemiluminescent enzyme-linked immunosorbent assay (MB-CLEIA) with high sensitivity, wide detection range, ultra-short detection time, and multiple suitability was developed. For the first anti-AFB_1, nanobody was screened from an immunized phage-display antibody library, and Nb and ALP-Nb were prepared by *Escherichia coli* expression system. Our work showed the interaction between AFB_1 and nanobody by molecular docking, and we found sequence of Nb and ALP would greatly affect the activity of Nb10E; the format as ALP-linker-Nb showed good binding activity to AFB_1·BSA and AFB_1 molecule, while the Nb-linker-ALP only had the binding activity to AFB_1·BSA, since the ALP was too close to the complementarity determining region (CDR) 3 domain of Nb10E, which would affect the interaction of AFB_1 molecule. After optimization, the developed method could achieve the ultrasensitive detection of AFB_1 with LOD = 0.743 pg mL^{-1} and IC_{50} = 0.33 ng mL^{-1}, and the linear range was from 0.00723 ng mL^{-1} to 12.38 ng mL^{-1}, and showed powerful tolerance and utility for complex matrix environments in sample detection, which only need simple dilution and the recoveries were from 96.24 to 123.37% in oats, corn, and oil sample. What is even more remarkable is that all detection time, including sample pretreatment, incubation, and measure, only need 30 min, which would greatly improve the timeliness and would offer a promising strategy for application of other nanobody.

Experimental

Materials and reagents

AFB_1·BSA and AFB_1 were purchased from Ludubio Ltd (Shandong, China). Camel Peripheral Blood Lymphocyte Isolate Kit was acquired from Solarbio Ltd (Beijing, China). PrimeScript™ IV 1st strand cDNA Synthesis Mix was sourced from TaKaRa (Beijing, China). Restriction endonucleases X-MAI, KpnI-HF, T4 DNA ligase and Q5 High-Fidelity DNA Polymerase were obtained from New England Biolabs Ltd. (Beijing, China). The Trans5α and TransB (DE3) Chemically competent Cell was sourced from TransGen Biotech Ltd (Beijing, China). Ni-NTA Sefinose™ Resin (Settled Resin) was purchased from Sangon Biotech (Shanghai, China). Anti-His-tag mAb-HRP-DirecT was purchased from Medical & Biological Laboratories Ltd (Japan). Epoxy-magnetic beads, alkaline phosphatase substrate (APS-5) and blocking buffer were obtained from BioMag Ltd (Wuxi, China). Corning 96-well White Flat Bottom Polystyrene High Bind Microplates were purchased from CORNING Incorporated (USA). The chemiluminescence immunoanalyzer SpectraMax-5M was produced from Molecular Devices Inc. (USA).

ALP-Nb fusion protein preparation

To construct a specific nanobody library against AFB_1, a healthy camel was subcutaneously immunized three times with emulsified complete antigen [AFB_1·BSA (1 mg mL^{-1}), 1 mL AFB_1·BSA + 1 mL saline + 2 mL incomplete adjuvant] at an interval of 1 week. Nanobody titer was estimated by indirect ELISA (iELISA). Four to five days after the third immunization, the peripheral blood lymphocytes were

isolated from a 20 mL fresh and frozen blood sample. Total RNA was obtained from lymphocytes and reverse transcribed to cDNA, and then VHH fragments were obtained by polymerase chain reaction (PCR) using cDNA. The fragments of VHH were ligated into the phagemid vector pCantab 5E (digested by the restriction enzyme KpnI-HF and XmaI). Then recombinant phageminds (VHH-pCantab 5E) were electroporated into the pre-prepared *Escherichia coli* (*E. coli*) *TG1* electroporation-competent cells. At last, after VHH library has been successfully constructed, anti-AFB_1 nanobodies were screened by 4 rounds of bio-panning using iELISA, during the screening process, phages expressing VHH was added to the coated wells for shaking incubation and forcefully washed ten times with PBST (PBS containing 1% tween-20, v/v), and then eluted using AFB_1 molecule. *E. coli TG1* was infected by eluted phages and cultured at 37 °C, from which 96 colonies were randomly selected and cultured separately, and then indirect competitive ELISA (icELISA) was used to identify the sensitivity of each single colony [23]. The anti-AFB_1 nanobody genes obtained from the bio-panning were digested and ligated into the pET-22b vector at the same restriction site, named the pET-22b-VHH vector. The *E. coli strain Trans B (DE3)* was used to express above nanobody proteins, which were induced at 16 °C with Isopropyl-beta-D-thiogalactopyranoside (IPTG, 0.1 mM) for overnight. VHH proteins were directly purified by Ni-NTA column. To evaluate the sensitivity of expression and purification products, icELISA with anti-His tag monoclonal antibody (mAb) was applied.

ALP-Nb fusion fragments were constructed by fusing ALP (derived from *E. coli*) and (G4S) 3 linker and nanobodies by gene splicing by overlap extension polymerase chain reaction (SOE-PCR) [24]. Then, ALP-Nb fusion protein was expressed and purified in the same way as nanobody proteins and identified by sodium dodecyl sulfate–polyacrylamide gel electrophoresis (SDS-PAGE), and the concentration determination of purified ALP-Nb was performed by bicinchoninic acid protein quantification (BCA assay). ALP-Nb was demonstrated by one-step indirect competitive chemiluminescent enzyme-linked immunosorbent assay (icCLEIA) using the chemiluminescence intensity (CL intensity) of ALP and APS-5 (the main components and the principle action of APS-5 are shown in Support information Fig. 8) as signal output.

Preparation of AFB_1·BSA immunomagnetic beads

0.2 mL Epoxy-magnetic beads (Epoxy-MBs) (20 mg mL^{-1}) was injected into a 1.5 mL EP tube. Epoxy-MBs were placed in a magnetic field to separate and washed three times with 0.5 mL of PBS buffer (0.1 mM, 1 mM EDTA, pH 8.5). Then, Epoxy-MBs were mixed in 1 mL PBS buffer containing 0.15 mg AFB_1·BSA and 185 mg Na_2SO_4, meanwhile, a control group without AFB_1·BSA was established and named as negative Epoxy-MBs (N-MBs). Two kinds of mixtures were shaken gently for 12 h at room temperature and washed three times with 0.5 mL of PBS buffer. After that, the MBs were blocked by magnetic beads blocking buffer for 6 h and washed six times with 1.0 mL PBST buffer to obtain AFB_1·BSA-MBs (AFB_1-MBs) and N-MBs.

Establishment of the MB-CLEIA

Series of concentrations of ALP-Nb was used to titrate AFB_1-MBs. AFB_1 molecule/reaction solution, ALP-Nb and AFB_1-MBs/N-MBs were mixed in reaction solution, then simultaneously added to the white ELISA-wells with nonbinding surface and incubated at 37 °C, and collection of ALP-Nb-AFB_1-MBs/N-MBs was performed by magnetic adsorption, while free AFB_1 and ALP-Nb-AFB_1 were washed with PBST. After that, 100 µL APS-5 was added to the reaction bath and the CL intensity of ALP-Nb bound to AFB_1-MBs and CL intensity of negative control were monitored using SpectraMax-5M.

Optimization of the MB-CLEIA

To achieve optimal performance of the MB-CLEIA, a range of testing influencing factors were adopted to optimize the detection condition under the premise that the total volume of the MB-CLEIA was determined to be 200 µL (volume ratio of diluting solution, ALP-Nb:AFB_1-MBs:AFB_1 = 3:4:3) [25–27]. Specifically, Epoxy-MBs diameters (0.3, 1.0, and 2.6 µm), the concentration of AFB_1-MBs (0.0625, 0.125, 0.25, and 0.5 mg mL^{-1}), amount of tested ALP-Nb (0.24 µg, 0.12 µg, 0.06 µg and 0.03 µg of ALP-Nb), reaction time (5, 10, 20, 40 and 80 min), times of washing (1, 2, and 3), thermal stability of ALP-Nb (0, 10, 20, 30, 40, and 50 min at 75 ℃), methanol content of AFB_1 PBS diluent (10%, 30%, and 60%, v/v), pH value (pH = 1.0, 2.0, 4.0, 6.0, 8.0, 10.0, and 12.0 of reaction solution), the concentration of NaCl (0, 25, 50, 100, 200 and 400 mM of reaction solution) were optimized and screened by comparing the CL intensity and the inhibition ratio of 0.5 ng mL^{-1} AFB_1 [Inhibition ratio (%) = (CL intensity of 0.5 ng mL^{-1} AFB_1 − CL intensity of negative control)/(CL intensity of 0 ng mL^{-1} AFB_1—CL intensity of negative control) × 100%]. Non-specific adsorption of MBs with ALP-Nb was analyzed using blocked N-MBs as a negative control.

Specificity

The specificity of MB-CLEIA, expressed as inhibition rate (IR), was certified by assessing the recognitional capacity of structural analogues, such as AFB_2, AFG_1, AFG_2, AFM_1, FB_1, DON, ZEN and T_2. IR (%) was expressed as

the inhibition rate of same concentration of the target analyte and analogue.

MB-CLEIA in samples

Sample detection capability of MB-CLEIA was confirmed by recovery rate of target standard addition and relative standard deviation. First, the impact of matrix effects on the detection system is assessed. 20 mL of 60% methanolic PBS was added to 5 g oats/corn and 5 ml of 60% methanolic PBS was added to 1 g oil, shaken vigorously at room temperature and centrifuged at 6000 g, and the supernatant was collected. Then, the supernatant was diluted onefold with PBS as AFB_1 diluent to compare the effect of different sample supernatants and 30% methanolic PBS on the CL intensity and the inhibition rate of 1 ng mL^{-1} AFB_1 in the detection system. AFB_1 standard (AFB_1 in methanolic solution, 10 μg mL^{-1}, 1 μg mL^{-1}, 0.1 μg mL^{-1}, and 10 ng mL^{-1}) in different concentrations were spiked in corn/oats/oil samples (spiked concentrations were 0.08, 0.4, 0.8, 8 and 80 μg kg^{-1}, according to the IC_{20}, IC_{50} and IC_{80} in the detection system standard curves), and extracted by adding 60% methanolic PBS; extracted samples were analyzed 5 times. The addition recovery rate (Recovery, %) and relative standard deviation (RSD, %) were calculated in the light of the following mathematical formula: Recovery ± SD (standard deviation) (%) = [(Measured value/Spiked value) ± SD] × 100% and RSD (%) = (standard deviation/average value) × 100%.

Results and discussion

Anti-AFB_1 nanobody acquisition

Nanobody has been applied in immunoassays, which can be screened to obtain by several rounds of bio-panning. The titer of nanobody against AFB_1 reached 1:5000 after immunizing three times with AFB_1·BSA. The total RNA was isolated from immune lymphocytes and reverse transcribed into cDNA that was amplified to the heavy chain antibody gene fragments of 750 bp in the first-round PCR (Support information Figure 1. (A)). After that, nanobody gene fragments about 450 bp (Support information Figure 1. (B)) was amplified in the second PCR, when everything was ready, the phage-display library against AFB_1 was successfully constructed and its capacity reached about 6×10^7 CFU mL^{-1}. Colony PCR results showed that VHH gene insertion rate reached 90% and gene sequencing analysis revealed good library diversity. During the four rounds of bio-panning, the coating concentration of AFB_1·BSA antigen decreased round by round (1 μg/well ~ 0.2 μg/well), specific phage bound to AFB_1·BSA was eluted using Glycine-Tris–HCl (pH 2.5, 1.0 M Tris–HCl, 0.75% Glycine, v/v) solution in the first and second bio-panning rounds, and then competitively eluted using AFB_1 molecule in the third and fourth bio-panning rounds (Support information Figure 2). Finally, three different Nbs were selected and named Nb10E, Nb81C, Nb12E (Support information Figure 3). Furthermore, Nb10E was found to show a high sensitivity with AFB_1 by icELISA, and the result showed that IC_{50} was 1.36 ng mL^{-1} and the linear range was 179.64 pg mL^{-1} ~ 13.33 ng mL^{-1} (Fig. 1A).

Structure simulation and docking analysis of Nb10E nanobody and AFB_1

The amino acid sequence of Nb10E was submitted to the Swiss-Model online homology modeling website, and then template searching with the help of Search for Templates (the sequence identity of the templates used in this study was generally not less than 60%), 20 templates were finally selected by X-ray method (resolution less than 2.0 Å) for homology modeling and construction of 3D structures and optimized using the OPLS-AA/L force field of GROMACS. The AFB_1 structural formula was downloaded from the Pubchem organic small-molecule bioactivity database and successfully completed the virtual screening using AutodockVina, resulting in the highest scoring conformation of the modeling template which was selected to construct the complex model, and named this template Model 8 (Fig. 1C). Ramachandron profiling of Model 8 (Fig. 1B) showed that 92.8% of the amino acids were located in the core region, indicating the reasonable optimized Nb10E structure. Molecular docking results showed that AFB_1 could bind to the nanobody active pocket through the Pi-Pi T-shape with PHE49; Van der Waals force with CYS45/MET46/GLY47/GLY59/ALA61/ILE63/TYR71/TYR72/ALA73/CYS121/PRO122/GLU127; carbon hydrogen bonds with GLN124/GLY62; Pi-Alkyl with TYR128 (Fig. 1D). At the same time, it can be learned that all three CDRs of Nb10E play an important role in the capture of AFB_1 which was wrapped in pocket-like CDR.

Preparation of ALP-Nb

The process of ALP-Nb expression vector construction is shown in Support information Fig. 4. After gene sequencing analysis (Azenta, Tianjin, China) (Support information Figure 5), the correctly constructed plasmids were transformed into *E. coli Trans B* (*DE3*). Fusion proteins were purified using Ni-NTA after induction of expression and analyzed using SDS-PAGE. The SDS-PAGE analysis showed that the fusion protein was soluble and had a band of approximately 70 kDa (Support information Figure 6). The result of BCA assay showed the concentration determination of purified ALP-Nb was 0.9966 μg $μL^{-1}$. In the course of the experiment, it was found that the competitive activity of linking

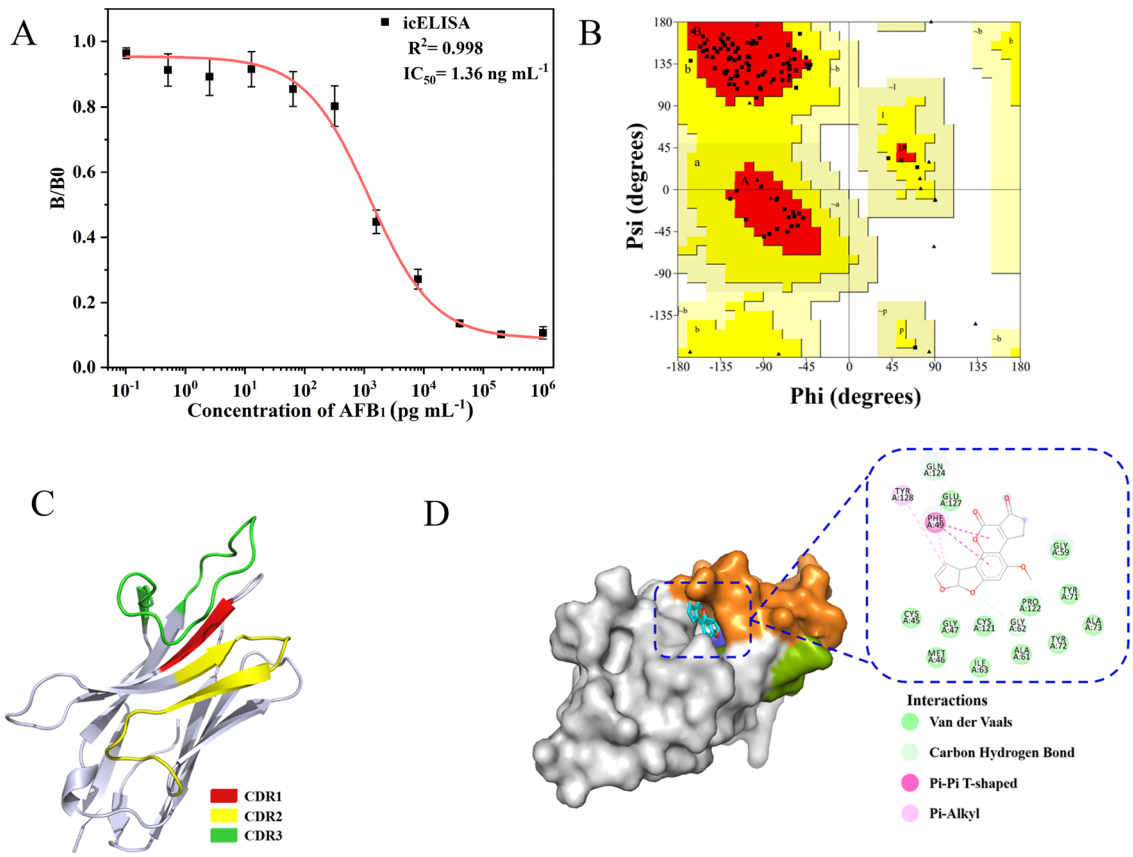

Fig. 1 **A** The sensitivities of Nb10E. **B** Ramachandron Plot. **C** Model 8 structure of CDR regions in Nb10E nanobody. **D** 3D and 2D interaction model of AFB_1 docking to Nb10E

ALP to the N terminus (ALP-Nb) of the Nb gene fragments was significantly better than that of linking to the C terminus (Nb-ALP), and icCLEIA were employed to compare the sensitivity of the two. The results showed that there was higher sensitivity for the free AFB_1 molecule when ALP-Nb was used (Support information Figure 7). We surmised that the relatively tiny size of the nanobodies is an important reason for the poor sensitivity of Nb-ALP, and it may affect the recognition of nanobody to AFB_1 and thus lead to a decrease in sensitivity. In contrast, the fusion of ALP-Nb moved away from CDRs, which facilitated exposure of the optimal region for antigen recognition. This discovery provides a viable avenue for the fusion expression or modification of antibodies with other signaling components, avoiding the compromise of the antibody's own properties (Scheme 1).

AFB_1·BSA-modified Epoxy-magnetic beads

Epoxy groups [–CH(O)CH–] have the ability to react with polyfunctional compounds to form cured products with cross-linked structures, and they are able to undergo ring-opening reactions with sulfhydryl groups to combine thioethers under mild conditions, due to the presence of high tension in the ternary ring [28]. BSA, a free sulfhydryl group is located at position 34 of the BSA peptide chain. Therefore, AFB_1·BSA can be modified on the surface of epoxy-based magnetic beads (Epoxy-MBs), three different particle sizes of MBs (0.3, 1.0, 2.6 μm) were modified with AFB_1·BSA under the same reaction conditions. As shown in Fig. 2A, compared to the Epoxy-MBs (− 32.03 mV), AFB_1-MBs showed a negative charge (− 38.83 mV) after modifying AFB_1·BSA (− 20.43 mV), and negative-MBs (− 17.2 mV) showed a clear change; after the binding of ALP-Nb to AFB_1-MBs, a new negative charge (− 11.73 mV) was likewise revealed, and these fully confirmed that AFB_1-BSA was successfully immobilized on the surface of Epoxy-MBs. Moreover, the slight change in the DLS further proved the successful immobilization of AFB_1-BSA onto Epoxy-MBs (Fig. 2B). Taking 0.3 μm MBs as an example, field emission scanning electron microscopy (SEM) images revealed that the epoxy-based magnetic beads were clustered with coarse surfaces and average diameters of approximately 0.3 μm, and the rough surfaces of the beads were beneficial for labeling biomolecules; on the contrary, the AFB_1-MBs were monodispersed and homogeneous, with smooth surfaces. The detailed structure in the inset of Fig. 2C, D shows

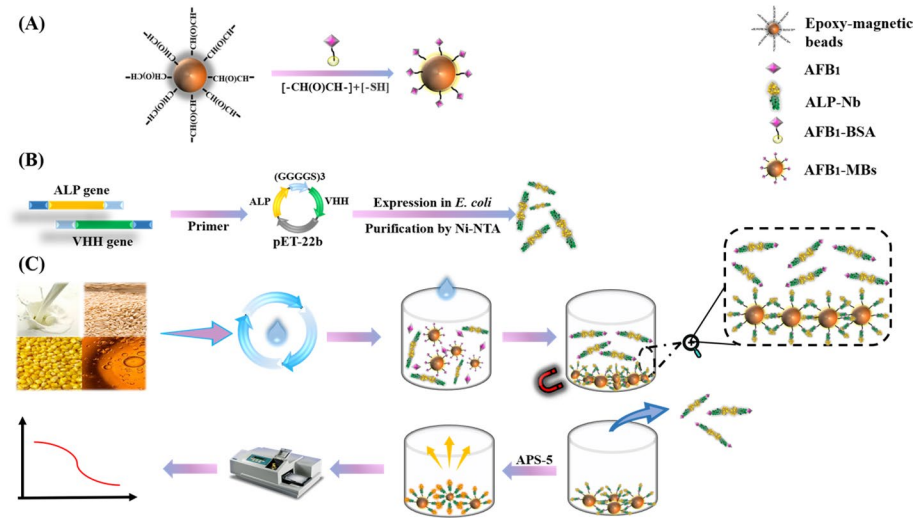

Scheme 1 **A** Synthesis of AFB_1-magnetic beads (AFB_1-MBs). **B** Synthesis of alkaline phosphatase-nanobody (ALP-Nb). **C** Schematic of magnetic separation competitive immunoassay assay for AFB_1 detection

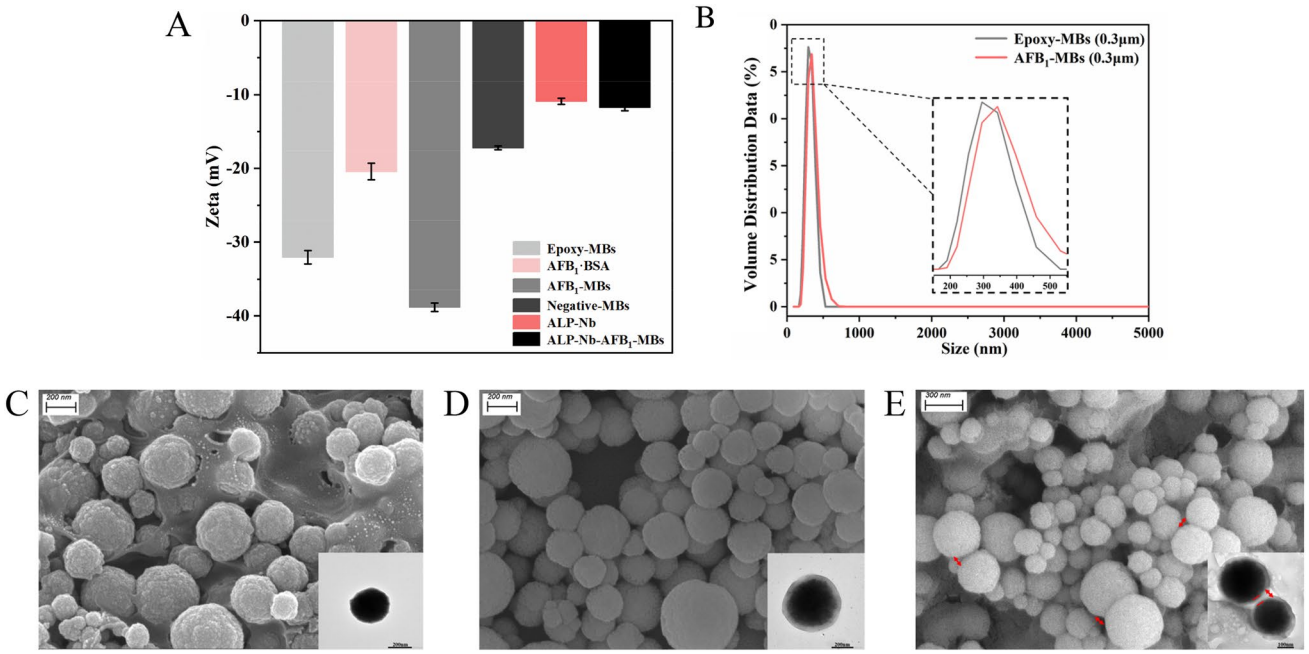

Fig. 2 **A** Zeta potential of Epoxy-MBs, AFB_1·BSA, AFB_1-MBs, Negative-MBs, ALP-Nb and ALP-Nb- AFB_1-MBs. **B** DLS of Epoxy-MBs and AFB_1-MBs. **C** SEM image of 0.3 μm Epoxy-magnetic beads. Inset: TEM image of 0.3 μm Epoxy-magnetic beads. **D** SEM image of 0.3 μm AFB_1-MBs. Inset: TEM image of 0.3 μm AFB_1-MBs. **E** SEM image of 0.3 μm ALP-Nb-AFB_1-MBs. Inset: TEM image of 0.3 μm ALP-Nb-AFB_1-MBs

that clear edges and uneven surfaces of MBs by field emission transmission electron microscope (TEM), and blurred edges of AFB_1-MBs. The TEM images showed sizes and surface morphologies, which were consistent with the SEM results. ALP from *E. coli* is a dimer composed of identical monomers [29, 30]. Figure 2E shows that a fixed-size gap was formed between AFB_1-MBs bound to ALP-Nb, and the fixed-size gap was indicated by the red arrow; the above phenomenon was more obvious in the TEM illustrations.

Optimization of the detection system

A wide variety of factors affect the performance of MB-CLEIA. The appropriate AFB_1-MBs and ALP-Nb content is essential for improving the sensitivity of the reaction system. The results showed that 0.3 μm, 1.0 μm and 2.6 μm AFB_1-MBs at concentrations of 0.25 mg mL^{-1}, 0.0625 mg mL^{-1} and 0.25 mg mL^{-1}, respectively, showed the optimal inhibition rate of AFB_1 (1.0 ng mL^{-1}) with

0.24 µg tested ALP-Nb (Fig. 3A, B, C). Particle size of the AFB_1-MBs affects the stability and density of the antibody/antigen binding. After the dosage of AFB_1-MBs and ALP-Nb in MB-CLEIA was determined, three standard curves of different AFB_1-MBs particle sizes were established (Fig. 3D, E, F). Obviously, the standard curve comparison showed that 0.3 µm of MBs achieved the best sensitivity under the same conditions (the linear range was 0.0372–4.314 ng mL^{-1}, IC_{50} was 0.422 ng mL^{-1}).

The co-incubation time of ALP-Nb, AFB_1-MBs, and AFB_1 in MB-CLEIA was called reaction time, which was the time required for antibody to recognize and bind to the target, and reaction time and number of washings were optimized in order to improve the sensitivity and at the same time reduce the detection time. Reaction system was incubated at 37 °C for 5, 10, 20, 40 and 80 min. The results showed that the reaction reached a maximum CL intensity at 20 min, and the sensitivity was expressed by the inhibition ratio, which means ALP-Nb has sufficiently bound to the target, still stable at 40 and 80 min (Fig. 4A). Therefore, the incubation time of the reaction was set to 20 min, which saved a lot of time compared with traditional ELISA and other methods, probably because the liquid phase detection environment provided by MB-CLEIA was more conducive to the performance of the antibody.

Subsequently, the number of post-reaction washes was optimized, the free samples were eluted and ALP-Nb-AFB_1-MBs were adsorbed at the bottom of the reaction cell by magnetic enrichment, and eluted 1, 2, and 3 times using PBST, respectively. The results showed that the better CL intensity and detection sensitivity were exhibited when the number of washes was 1 time (Fig. 4B). In summary, MB-CLEIA ensured better sensitivity while greatly reducing the detection time, from sample addition to result acquisition in 30 min. Moreover, the operation process was simple and convenient.

In order to equip MB-CLEIA with the ability to cope with the complex and uncontrollable assay environment, standard curves were established in three different concentrations of methanolic solutions (Fig. 4C, D, E). The IC_{50} was closer in 10% and 30% methanolic PBS buffer (v/v), but the linear range of detection was greater in 30% methanolic PBS buffer (v/v). Then, pH and salt concentration were optimized (Fig. 4G). All other conditions being equal, CL intensity was maximum in reaction solution at pH 8.0, and under this condition, MB-CLEIA has the lowest inhibition ratio; this means that the sensitivity of MB-CLEIA is highest at pH 8.0. Same as above, NaCl was added to the PBS buffer to prepare different concentrations of salt reaction solution (Fig. 4H). MB-CLEIA has superior sensitivity in 200 mM NaCl reaction solution. High

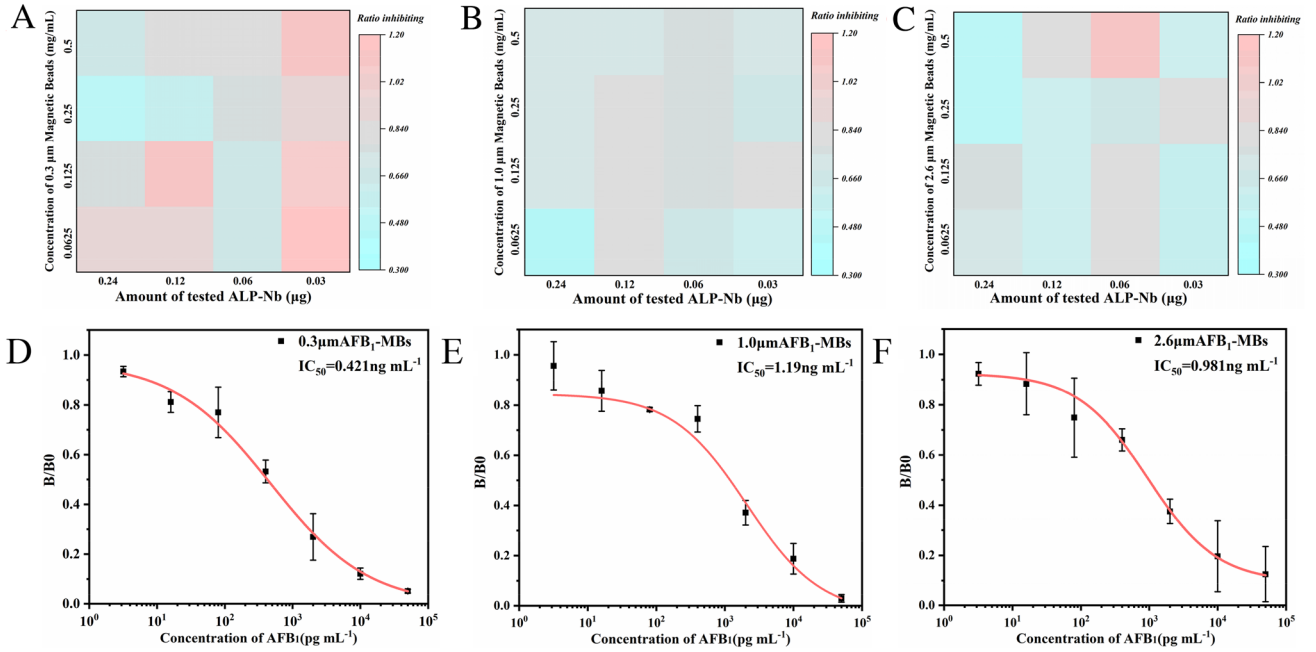

Fig. 3 **A** The concentration of 0.3 µm AFB_1-MBs and amount of tested ALP-Nb were optimized for detecting AFB_1 (1 ng mL^{-1}). **B** The concentration of 1.0 µm AFB_1-MBs and amount of tested ALP-Nb were optimized for detecting AFB_1 (1 ng mL^{-1}). **C** The concentration of 2.6 µm AFB_1-MBs and amount of tested ALP-Nb were optimized for detecting AFB_1 (1 ng mL^{-1}). **D** Calibration curves established with 0.3 µm AFB_1-MBs. **E** Calibration curves established with 1.0 µm AFB_1-MBs. **F** Calibration curves established with 2.6 µm AFB_1-MBs

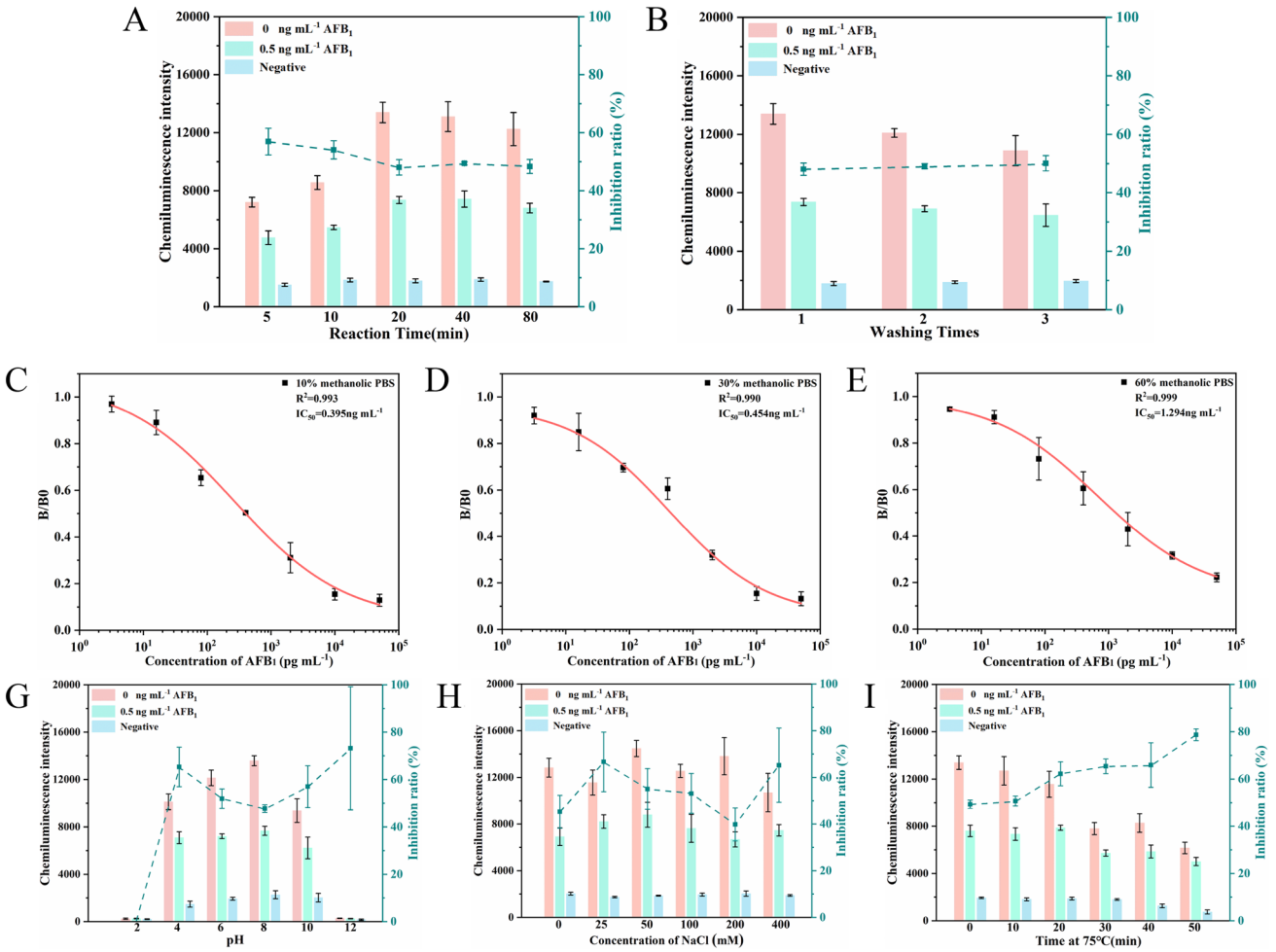

Fig. 4 **A** Reaction incubation time at 37 °C for 5, 10, 20, 40 and 80 min. **B** Times of washing (1, 2, 3). **C** Calibration curves established with Methanolic PBS buffer (10%) as AFB_1 dilution reagent. **D** Calibration curves established with Methanolic PBS buffer (30%) as AFB_1 dilution reagent. **E** Calibration curves established with Methanolic PBS buffer (60%) as AFB_1 dilution reagent. **F** Different pH reaction solution. **G** Different concentration of NaCl reaction solution. **H** Incubated at 75 ℃ for 0, 10, 20, 30, 40 and 50 min

NaCl concentrations are present in many samples, so the salt tolerance of the assay is very valuable. The thermostability of an antibody reflects its ability to maintain its activity under extreme temperatures conditions or after repeated multiple freeze–thaw [31–33]. Finally, we found in the thermostability experimental results that ALP-Nb still had high activity and was incubated for 20 min at 75 °C; both the binding ability of Nb to the target and the ALP-catalyzed chemiluminescence activity of APS-5 were relatively stable (Fig. 4I). After optimization, the detection sensitivity of MB-CLEIA has been further improved, and the powerful tolerance of temperature, acid–base and salt concentration allow our method to be better applied to sample detection, and also show the strong application prospects.

Magnetic separation immunoassay for AFB_1 based on ALP-Nb10E

Under the optimized experimental conditions, the MB-CLEIA was performed to analyze various concentrations of AFB_1 through chemiluminescence signal amplifier readout. Due to the non-specific binding of MBs and ALP-Nb, a slight background value was observed, to exclude this effect, the CL intensities of Negative-MBs have been subtracted from the CL intensities of different concentrations of AFB_1. Figure 5A shows the relationship between the CL intensity and AFB_1 concentration. As expected, compared with conventional ELISA (Fig. 1A), MB-CLEIA obviously enhanced the sensitivity, reduced analysis time, and also revealed a relatively wide detection range. Under the same reaction conditions, for icCLEIA-based

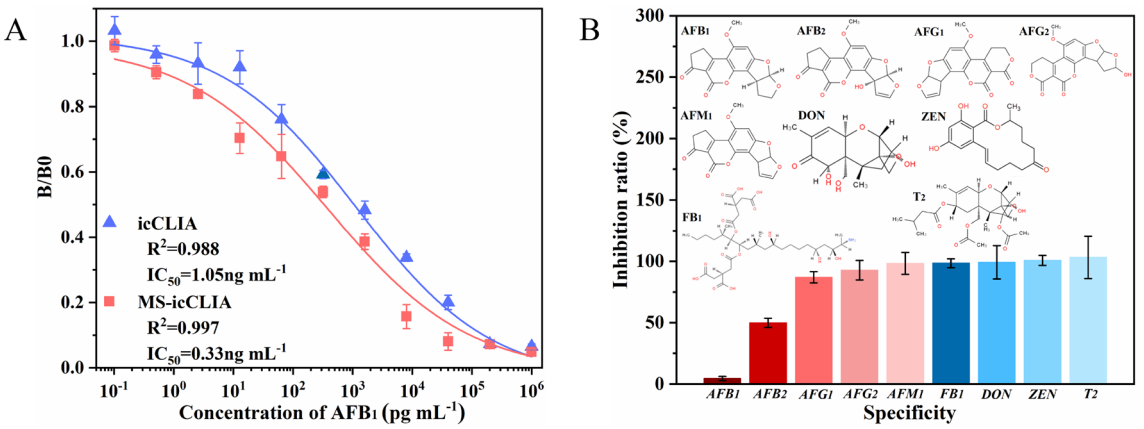

Fig. 5 **A** Calibration curve for AFB_1 detection with concentration range from 0 to 10^6 pg mL^{-1}. **B** Specificity evaluation for magnetic separation immunoassay, including AFB_1, AFB_2, AFG_1, AFG_2, AFM_1, FB_1, DON, ZEN and T_2 (all were 50 ng mL^{-1})

ALP-Nb10E, IC_{50} was 1.05 ng mL^{-1}, and the linear range was 35.13 ~ 28.205 ng mL^{-1}. For MB-CLEIA, the LOD was 0.743 pg mL^{-1} (IC_{90}), IC_{50} was 0.33 ng mL^{-1}, and the linear range was 7.23–12.38 ng mL^{-1} (IC_{20} ~ IC_{80}). Briefly, the method we developed was confirmed to be an efficient sensitive and timesaving immunoassay for AFB_1.

Specificity

As a quick and sensitive immunoassay, specificity was the critical parameter for evaluating MB-CLEIA. Including AFB_1, aflatoxin B_2 (AFB_2), aflatoxin G_1 (AFG_1), aflatoxin G_2 (AFG_2), aflatoxin M_1 (AFM_1), fumonisin B_1 (FB_1), deoxynivalenol (DON), Zearalenone (ZEN) and trichothecenes-2 (T_2) (50 ng mL^{-1}), MB-CLEIA was challenged with a series of interfering analogues. Specificity was calculated by the inhibition rate of the analogue. It was clear that the inhibition rate generated by different interfering analogue was higher compared to AFB_1. The above-mentioned experiments demonstrated that MB-CLEIA did not show specific recognition performance with the structural analogues of AFB_1 (Fig. 5B).

Matrix effect

Matrix compounds such as proteins, fats, sugars and pigments are present in most samples. Aforementioned substances may affect direct detection due to their unavoidable and unpredictable matrix effects. MB-CLEIA should not only have superior performance, but also be able to withstand complex testing environments. Therefore, we first examined the influence of the sample matrix on our method. 60% methanolic PBS was added to the samples with vigorous shaking, and then the supernatant was collected by centrifugation, which was the blank extraction solution. Blank extracting solutions were diluted one-, four-, and tenfold containing 0.5 ng mL^{-1} AFB_1. The CL intensity and sensitivity of different matrix solutions were compared with those of the 30% methanolic PBS. It was noticed that the CL intensity and detection sensitivity maintained relative stability when the dilution of sample matrix was one-, four-, and tenfold (Fig. 6A, B, C). In other words, when the extracts were onefold diluted, the MB-CLEIA showed the same sensitivity as under the optimal conditions.

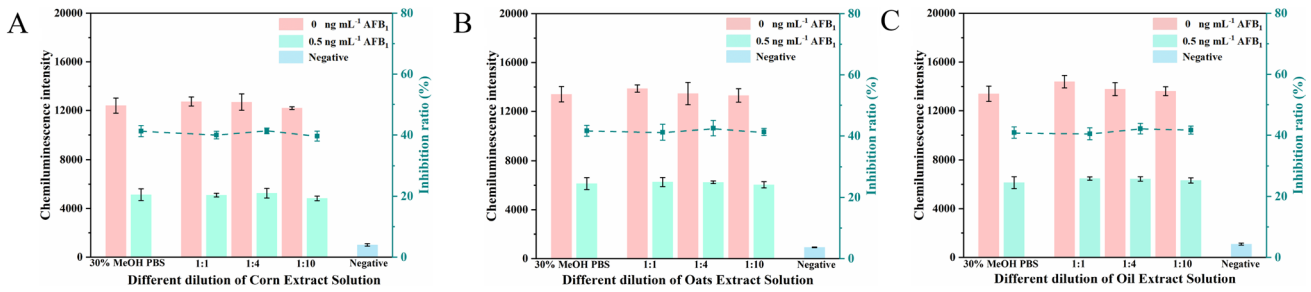

Fig. 6 **A** Matrix effect of corn. **B** Matrix effect of oats. **C** Matrix effect of oil

Table 1 Recovery analysis of AFB_1 spiked in samples (corn, oats, and oil) using magnetic separation competitive immunoassay ($n=5$)

Sample	Spiked concentration (μg kg^{-1})	Recovery ± SD (%)	RSD (%)
Corn	0	–	–
	8×10^{1}	101.05 ± 3.56	3.52
	8×10^{0}	100.52 ± 3.04	3.03
	8×10^{-1}	81.75 ± 3.79	4.64
	4×10^{-1}	85.16 ± 6.18	7.26
	8×10^{-2}	120.30 ± 3.60	2.99
Oats	0	–	–
	8×10^{1}	103.96 ± 4.02	3.87
	8×10^{0}	97.15 ± 1.70	1.75
	8×10^{-1}	88.95 ± 4.11	4.62
	4×10^{-1}	92.15 ± 2.28	2.48
	8×10^{-2}	92.42 ± 1.30	1.40
Oil	0	–	–
	8×10^{1}	103.21 ± 4.72	4.57
	8×10^{0}	102.32 ± 2.29	2.24
	8×10^{-1}	98.56 ± 5.66	5.74
	4×10^{-1}	113.23 ± 12.41	10.96
	8×10^{-2}	122.25 ± 14.56	11.91

Table 2 Overview and comparison of developed immunoassays for the detection of AFB_1

Detection method	LOD (ng mL^{-1})	Liner range (ng mL^{-1})	Time (min)	Antibody	Ref
Time-resolved fluorescence immunochromatographic assay	0.05	0.13 ~ 4.54	–	AldNb, mAb	[34]
Biotin-streptavidin-amplified enzyme-linked immunosorbent assay	0.04	0.08 ~ 0.65	50	Nb	[35]
Nanobody-based enzyme immunoassay	–	0.117 ~ 5.676	–	Nb	[36]
A label-free electrochemical immunosensor	8.43×10^{-5}	3.12×10^{-4} ~ 1.56×10^{-3}	> 90	Nb	[37]
Electrochemical competitive immunosensor	6.8×10^{-5}	0.5 ~ 10	120	Nb	[38]
Homogeneous immunosensor	0.04	0.06 ~ 5	20	mAb	[39]
Bienzymatic chemiluminescence competitive immunoassay	5×10^{-6}	–	> 40	mAb	[40]
Our work	7.34×10^{-4}	7.23×10^{-3} ~ 12.38	30	Nb	–

Samples testing

The specific, rapid and sensitive properties of MB-CLEIA had to be applied to the detection of AFB_1. The recovery tests were performed by analyzing corn, oats, and oil samples spiked with six levels of AFB_1 (0, 0.08, 0.4, 0.8, 8, and 80 μg kg^{-1}). The results in Table 1 showed that the application performance of MB-CLEIA exhibited satisfying accuracy with the recovery of 96.24–123.37%. Briefly, these results indicated that MB-CLEIA has the ability to be used to effectively and accurately quantify AFB_1 in agricultural crops and their products.

Comparison of immunoassay methods for AFB_1

The immunoassays that have been successfully established and published for AFB_1 are shown in Table 2, compared to these immunoassays, MB-CLEIA exhibits advantages in terms of fast quantification of the test results, ultra-sensitivity, relatively wide linear ranges and ability to resist interference from complex detection environments.

Conclusions

To sum up, by the effective integration of chemiluminescent signal amplification output and fast magnetic separation technology into one entity, MB-CLEIA significantly improved the sensitivity and reliability of immunoassays. An ultrasensitive, specific, and stable magnetic separation immunoassay for AFB_1 based on ALP-Nb10E has been developed, and realized the goal of one step, in which detection procedures is simplified significantly. The test sample and the test reagent were added to the reaction cell at the same time, with a reaction time of 20 min and only one wash, the test can be completed within 30 min. Moreover,

our assay has the advantage of low cost and easy mass production due to the ease of preparation, mass expression and gene modification of Nb, and the cost of the MB-CLEIA was only 0.05 dollar per sample when the test consumption was tallied. In particular, our method exhibited high sensitivity towards AFB_1, with LOD 0.743 pg mL^{-1} and $IC_{50} = 0.33$ ng mL^{-1}. What is more valuable was that our assays showed superior analytical performance to cope with complex testing conditions, after excluding matrix effects, MB-CLEIA has the ability to detect corn, oats, and oil. This also means that the magnetic separation immunoassay based on ALP-Nb10E shows promising application in the field of rapid detection of AFB_1.

Supplementary Information The online version contains supplementary material available at https://doi.org/10.1007/s00217-023-04202-3.

Acknowledgements This research has received funding support from (20SWAQK16, 2019GGRC03, 2019CXTD03), Heilongjiang Province Key Laboratory of Microecology-Immune Regulation Network and Related Diseases (2021-SZD-JC-005), 2021 Heilongjiang Provincial Health and Wellness Committee Project (20210202040058)

Author contributions XW: conceptualization, writing—original draft, methodology, and writing—review and editing. WL: methodology, investigation, and software. HZ: investigation and methodology. WS: investigation and methodology. YZ: methodology and software. RL: methodology and validation. LG: investigation and validation. WW: investigation and validation. CS: writing—review and editing, supervision, and methodology. TS: investigation, writing—review and editing, validation, and funding acquisition.

Data availability The authors confirm that the data supporting the findings of this study are available within the article.

Declarations

Conflict of interest The authors declare no conflict of interest.

Ethical approval The research does not involve human participants.

References

1. Caceres I, Snini SP, Puel O, Mathieu F (2018) *Streptomyces roseolus*, a promising biocontrol agent against *Aspergillus flavus*, the main aflatoxin B1 producer. Toxins 10:442
2. Battilani P, Toscano P, Van der Fels-Klerx HJ, Moretti A, Camardo Leggieri M, Brera C, Rortais A, Goumperis T, Robinson T (2016) Aflatoxin B1 contamination in maize in Europe increases due to climate change. Sci Rep 6:24328
3. Streit E, Schatzmayr G, Tassis P, Tzika E, Marin D, Taranu I, Tabuc C, Nicolau A, Aprodu I, Puel O, Oswald IP (2012) Current situation of mycotoxin contamination and co-occurrence in animal feed–focus on Europe. Toxins (Basel) 4:788–809
4. Cimbalo A, Alonso-Garrido M, Font G, Manyes L (2020) Toxicity of mycotoxins in vivo on vertebrate organisms: a review. Food Chem Toxicol 137:111161
5. Mahato DK, Lee KE, Kamle M, Devi S, Dewangan KN, Kumar P, Kang SG (2019) Aflatoxins in food and feed: an overview on prevalence detection and control strategies. Front Microbiol 10:2266
6. Abrar M, Anjum FM, Butt MS, Pasha I, Randhawa MA, Saeed F, Waqas K (2013) Aflatoxins: biosynthesis, occurrence, toxicity, and remedies. Crit Rev Food Sci Nutr 53:862–874
7. Khayoon WS, Saad B, Lee TP, Salleh B (2012) High performance liquid chromatographic determination of aflatoxins in chilli, peanut and rice using silica based monolithic column. Food Chem 133:489–496
8. Romera D, Mateo EM, Mateo-Castro R, Gómez JV, Gimeno-Adelantado JV, Jiménez M (2018) Determination of multiple mycotoxins in feedstuffs by combined use of UPLC-MS/MS and UPLC-QTOF-MS. Food Chem 267:140–148
9. Chen F, Luan C, Wang L, Wang S, Shao L (2017) Simultaneous determination of six mycotoxins in peanut by high-performance liquid chromatography with a fluorescence detector. J Sci Food Agric 97:1805–1810
10. Wang X, Niessner R, Tang D, Knopp D (2016) Nanoparticle-based immunosensors and immunoassays for aflatoxins. Anal Chim Acta 912:10–23
11. Zhang D, Li P, Zhang Q, Zhang W (2011) Ultrasensitive nanogold probe-based immunochromatographic assay for simultaneous detection of total aflatoxins in peanuts. Biosens Bioelectron 26:2877–2882
12. Gazzaz SS, Rasco BA, Dong FM (1992) Application of immunochemical assays to food analysis. Crit Rev Food Sci Nutr 32:197–229
13. Du J, Chen X, Liu K, Zhao D, Bai Y (2022) Dual recognition and highly sensitive detection of *Listeria* monocytogenes in food by fluorescence enhancement effect based on Fe3O4@ZIF-8-aptamer. Sens Actuators B 360:131654
14. Zhang W, Serpe MJ (2017) Antigen detection using fluorophore-modified antibodies and magnetic microparticles. Sens Actuators B 238:441–446
15. Yue Q, Li X, Fang J, Li M, Zhang J, Zhao G, Cao W, Wei Q (2022) Oxygen Free Radical Scavenger PtPd@PDA as a dual-mode quencher of electrochemiluminescence immunosensor for the detection of AFB1. Anal Chem 94:11476–11482
16. Gonzalez-Sapienza G, Rossotti MA, Tabares-da Rosa S (2017) Single-domain antibodies as versatile affinity reagents for analytical and diagnostic applications. Front Immunol. https://doi.org/10.3389/fimmu.2017.00977
17. Shu M, Xu Y, Wang D, Liu X, Li Y, He Q, Tu Z, Qiu Y, Ji Y, Wang X (2015) Anti-idiotypic nanobody: a strategy for development of sensitive and green immunoassay for Fumonisin B_1. Talanta 143:388–393
18. Tang Z, Wang X, Lv J, Hu X, Liu X (2018) One-step detection of ochratoxin A in cereal by dot immunoassay using a nanobody-alkaline phosphatase fusion protein. Food Control 92:430–436
19. Ren W, Li Z, Xu Y, Wan D, Barnych B, Li Y, Tu Z, He Q, Fu J, Hammock BD (2019) One-step ultrasensitive bioluminescent enzyme immunoassay based on nanobody/nanoluciferase fusion for detection of aflatoxin B_1 in cereal. J Agric Food Chem 67:5221–5229
20. Dunlop EH, Feiler WA, Mattione MJ (1984) Magnetic separation in biotechnology. Biotechnol Adv 2:63–74
21. Wang F, Li ZF, Yang YY, Wan DB, Vasylieva N, Zhang YQ, Cai J, Wang H, Shen YD, Xu ZL, Hammock BD (2020) Chemiluminescent enzyme immunoassay and bioluminescent enzyme immunoassay for tenuazonic acid mycotoxin by exploitation of nanobody and nanobody-nanoluciferase fusion. Anal Chem 92:11935–11942
22. Di S, Ning T, Yu J, Chen P, Yu H, Wang J, Yang H, Zhu S (2020) Recent advances and applications of magnetic nanomaterials in environmental sample analysis. TrAC Trends Anal Chem 126:115864

23. Zhao F, Shi R, Liu R, Tian Y, Yang Z (2021) Application of phage-display developed antibody and antigen substitutes in immunoassays for small molecule contaminants analysis: a mini-review. Food Chem 339:128084
24. Sun T, Zhao Z, Liu W, Xu Z, He H, Ning B, Jiang Y, Gao Z (2020) Development of sandwich chemiluminescent immunoassay based on an anti-staphylococcal enterotoxin B nanobody-alkaline phosphatase fusion protein for detection of staphylococcal enterotoxin B. Anal Chim Acta 1108:28–36
25. Zhang YY, Li LH, Wang Y, Wang H, Xu ZL, Tian YX, Sun YM, Yang JY, Shen YD (2022) Ultrasensitive and rapid colorimetric detection of paraquat via a high specific VHH nanobody. Biosens Bioelectron 205:114089
26. Güttler T, Aksu M, Dickmanns A, Stegmann KM, Gregor K, Rees R, Taxer W, Rymarenko O, Schünemann J, Dienemann C, Gunkel P, Mussil B, Krull J, Teichmann U, Groß U, Cordes VC, Dobbelstein M, Görlich D (2021) Neutralization of SARS-CoV-2 by highly potent, hyperthermostable, and mutation-tolerant nanobodies. Embo j 40:e107985
27. Muyldermans S (2013) Nanobodies: natural single-domain antibodies. Annu Rev Biochem 82:775–797
28. Mateo C, Grazu V, Palomo JM, Lopez-Gallego F, Fernandez-Lafuente R, Guisan JM (2007) Immobilization of enzymes on heterofunctional epoxy supports. Nat Protoc 2:1022–1033
29. Hehir MJ, Murphy JE, Kantrowitz ER (2000) Characterization of heterodimeric alkaline phosphatases from *Escherichia coli*: an investigation of intragenic complementation. J Mol Biol 304:645–656
30. Sowadski JM, Handschumacher MD, Murthy HM, Foster BA, Wyckoff HW (1985) Refined structure of alkaline phosphatase from *Escherichia coli* at 2.8 A resolution. J Mol Biol 186:417–433
31. Kunz P, Zinner K, Mücke N, Bartoschik T, Muyldermans S, Hoheisel JD (2018) The structural basis of nanobody unfolding reversibility and thermoresistance. Sci Rep 8:7934
32. Le Basle Y, Chennell P, Tokhadze N, Astier A, Sautou V (2020) Physicochemical stability of monoclonal antibodies: a review. J Pharm Sci 109:169–190
33. Goldman ER, Liu JL, Zabetakis D, Anderson GP (2017) Enhancing stability of camelid and shark single domain antibodies: an overview. Front Immunol 8:865
34. Tang X, Li P, Zhang Q, Zhang Z, Zhang W, Jiang J (2017) Time-resolved fluorescence immunochromatographic assay developed using two idiotypic nanobodies for rapid, quantitative, and simultaneous detection of aflatoxin and zearalenone in maize and its products. Anal Chem 89:11520–11528
35. Yan T, Zhu J, Li Y, He T, Yang Y, Liu M (2022) Development of a biotinylated nanobody for sensitive detection of aflatoxin B(1) in cereal via ELISA. Talanta 239:123125
36. He T, Wang Y, Li P, Zhang Q, Lei J, Zhang Z, Ding X, Zhou H, Zhang W (2014) Nanobody-based enzyme immunoassay for aflatoxin in agro-products with high tolerance to cosolvent methanol. Anal Chem 86:8873–8880
37. Zhang X, Liao X, Wu Y, Xiong W, Du J, Tu Z, Yang W, Wang D (2022) A sensitive electrochemical immunosensing interface for label-free detection of aflatoxin B(1) by attachment of nanobody to MWCNTs-COOH@black phosphorene. Anal Bioanal Chem 414:1129–1139
38. Liu X, Wen Y, Wang W, Zhao Z, Han Y, Tang K, Wang D (2020) Nanobody-based electrochemical competitive immunosensor for the detection of AFB(1) through AFB(1)-HCR as signal amplifier. Mikrochim Acta 187:352
39. Xu W, Xiong Y, Lai W, Xu Y, Li C, Xie M (2014) A homogeneous immunosensor for AFB1 detection based on FRET between different-sized quantum dots. Biosens Bioelectron 56:144–150
40. Li J, Zhao X, Chen LJ, Qian HL, Wang WL, Yang C, Yan XP (2019) p-Bromophenol-enhanced bienzymatic chemiluminescence competitive immunoassay for ultrasensitive determination of aflatoxin B(1). Anal Chem 91:13191–13197